Single Antenna Positioning for smallest size breast Tumor Detection

MAZHAR B. TAYEL, HAZEM A. ELFAHAM

Abstract—It was previously proved the possibility of using SAR as a tool to detect tumor and its location in the breast as an organism in the human body. It is one of the most expressing quantitative metric parameters specifying electromagnetic (EM) wave energy absorption. The last work showed that the use of microstrip patch antenna (MSPA) as applicators for the modeled breast helps to determine the smallest tumor size. The dependency of EM absorption on the conductivity and permittivity of the tumor are main parameters that define tumor size and location. The present paper deals with studying and analyze of antenna positioning effect. The positioning represents a new trend for breast inspection to attain 2D and 3D imaging by searching the location of tumor taking slices of breast layers and performing a rotation around the breast.

Index Terms— anthropomorphic, body, location, plateau, position, SAR, size, slice layer, tilt, tumor.

1 Introduction

In the previous work given in [1, 2], modeling of breast tumor detection inspection system had been introduced. In this work, it was shown the possibility of using absorption of EM wave is a characteristic feature to discriminate normal tissue from tumor depending on their parameters (conductivity and permittivity). Also in this work, it was deduced new criteria feature parameters that determine the location and size of the tumor in the breast.

Objective of this paper is to study and analyze the effect of using the designed single MSPA in different positions as a slice layers along the major axis of the breast model for different scan angles around the breast for the purpose of determining probability of tumor existence and to determine its size and location using simulation of EM wave a propagation and absorption with the aid of the computer studio technique (CST), microwave studio which is a full-featured software package for electromagnetic analysis and design in the high-frequency range [3, 4].

2 The Proposed Antenna Positioning.

The positioning of antenna concerns with two main objectives, the first deals with a specified layer of the breast in a slice with a predetermine thickness and the second deals with antenna scanning around the studied slice.

(a) The proposed slice layer is taken equal to the designed MSPA length with no overlapping. Slices are selected along the length of the chamber major axis in five steps trials plus and additional position at the bottom (nipple).

(b) Slice layer scan the antenna assumed to rotate around the slice layer in steps (0^o, 90^o, 180^o, and 270^o) to study its effect on absorption.

In the study the tumor must have a nominated must have a nominated location to determine the smallest possible size to be detected depending on the slice layer position, antenna rotation angle and detectable tumor size.

2.1 The Proposed Inspection Chamber Structure.

The breast proposed container is a chamber of semi-ellipsoidal shape consisting of an FR-4 (lossy) material. The chamber structure shown in figure (1) and its dimensions are given in the table (1).

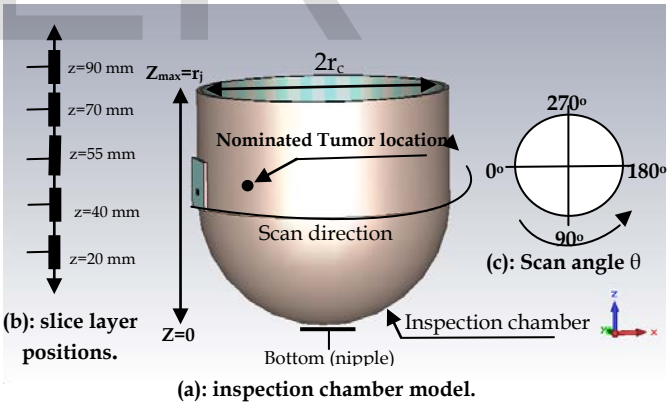

Fig. 1. The proposed structure of the inspection chamber and the proposed MSPA position(s) and scan angle direction.

Fig. 1 shows the proposed inspection chamber model with a diameter (2rc), and major axis rj, the assumed slice layer positions and the MSPA scan angles around the slice layer.

2.2 The Breast Model.

The breast is assumed as a semi-ellipsoid with a major axis r_J and minor radius r_b. The analyzed breast model consists of a fat layer that has a heterogeneous tissue, as shown in fig. 2 the skin layer is not included to reduce the complexity of the model and to reduce the simulation run time. The breast tissue includes a tumor at a nominated location(s) Q_n

- *Pr. Dr. /MAZHAR B. TAYEL, Ph.D. Supervisor, E E D, Faculty of Engineering, Alexandria University, Alexandria, Egypt, PH-01116554777. E-mail profbasyouni@gmail.com.*
- *HAZEM A. ELFAHAM is currently pursuing Ph.D. degree program in electric engineering in Alexandria University, Alexandria, Egypt, PH-01023471113. E-mail helfaham@gmail.com*

(x_n, y_n, z_n), as shown in fig. 1. The conductivity of the used materials was choosing as maximum as given in the table. 1 [5, 6].

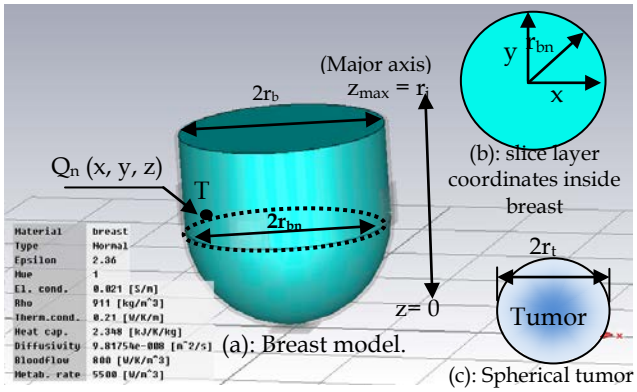

Fig. 2. The proposed coordinates of the slice layer in the breast.

TABLE 1
THE OBJECTIVE MATERIALS AND PARAMETERS

Item	Name		Symbol	Value
MSPA	Substrate length	(mm)	L	21.169
	Substrate thickness	(mm)	T	1.5
	Permittivity	(F/m)	ϵ	2.2
	Patch length	(mm)	L_p	9.78
	Patch width	(mm)	W_p	12.6
	Feed Rad	(mm)	R	0.48
	Feed offset	(mm)	L_o	1.5
Chamber	Permittivity	(F/m)	ϵ_c	4.3
	Major axis	(mm)	r_j	115
Breast	Permittivity	(F/ m)	ϵ_b	2.36
	Conductivity	(S/M)	σ_b	0.012
Tumor	Permittivity	(F/m)	ϵ_t	37.3
	Conductivity	(S/M)	σ_t	4

3 Measurement Parameters

The parameters to be measured are EM absorption at the nominated tumor location (SAR_{max}), its simulated location Q_s (x_s, y_s, z_s), and tumor size and the deviation δ between its nominated and simulated reactions. For the radiated energy from the single designed MSPA at different positions (slice layers) and angles (θ).

3.1 The specific Absorption Rate (SAR).

The specific absorption rate (SAR) is widely used for expressing quantities interactions of microwave electromagnetic (EM) energy with biological systems matter it must be used to determine the coordinate of simulated location Q_s (x_s, y_s, z_s), maximum SAR value within or outside a tumor and its size inside a breast tissue [7, 8, 9, 10].
The distribution plateau of specific absorption rate value (SAR) is:

$$SAR=\int \frac{\sigma(r)E^2(r)}{V\rho(r)}\,dr \quad (1)$$

Where: dr=r dΘ dΦ,
E(r) is the electric field (EF) profile,
σ(r) is the electric conductivity of the sample breast tissue or tumor,
ρ(r) is the density of the sample,
V is the partial volume covered by EF profile.

It is heavily depend on the size, geometry and effective volume mass of the part of the body exposed to RF energy of the micro strip patch antenna (MSPA) as a microwave source.
The EF profile exposed mass partial volume, thus SAR in tumor is spike.
Consequently, measurements are made for different slice positions along the scan angles around the specified breast slice layer.
Body partial exposed volume to EF profile, hence the effective conductivity:

$$\sigma_s = (\frac{\sigma_{br}}{V_{br}})V_s \quad (2)$$

Thus, anthropomorphic body of the EF lobe SAR plateau is formed.

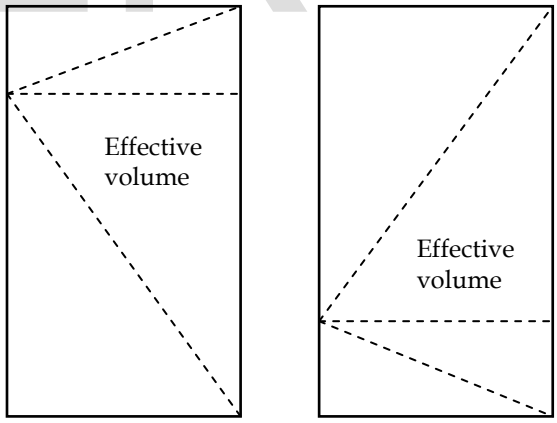

Fig. 3. The illustration mass volume.

Fig. 3 shows the illustration of the effective mass volume at two different points.

4 Experiments And Results.

In the following subsections introduces typical simulation experiments to be implemented for study and analyze the effect of antenna positioning on both, the anthropomorphic lobe body profile of far-field, and its EF distribution and its SAR plateau to determine the tumor absorption SAR $_{max}$ as well as its location and its minimum detectable size.

In the implementation in the following experiments tumor is located at a nominated coordinates Q_n (x_n, y_n, z_n) = Q_{60} (-30, 0, 60) with operation frequency 9GHz, MSPA, chamber, breast, and tumor constants are given in table (1).

4.1 Experiment-1.

Consider antenna position for the first slice layer is Z_{slice}=90mm, figure 3-a shows the obtained solution results for anthropomorphic lobe body profile and direction, figure 3-b shows the SAR plateau distribution as well as the spike of the absorption SAR_{max} detectable location at rotation angle θ=0°.

Table 2 gives the results for different tumor size according to the criteria for detectable tumor where the absorption SAR_{max} inside tumor spheres [2].

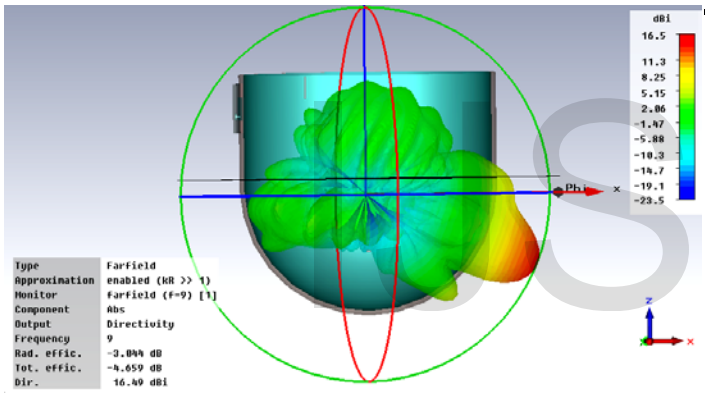

(a): The anthropomorphic far-field structure.

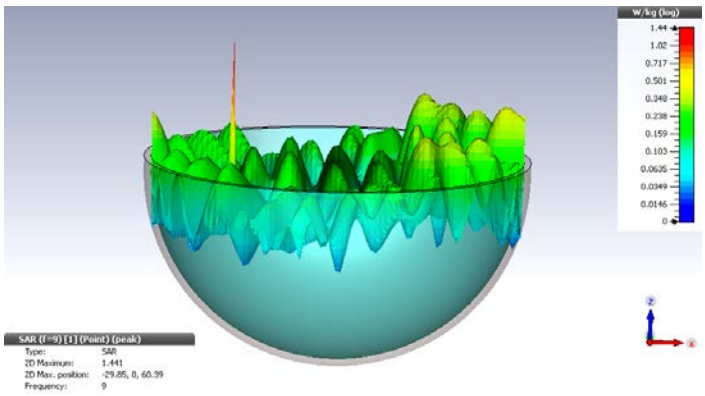

(b): SAR distribution profile for minimum size.

Fig. 4. The anthropomorphic far-field and SAR_{max} at minimum tumor size.

From fig. 4 it is evident that the anthropomorphic lobe body is directed downwards for bottom with the tilt angle Φ=-30, and from fig. 4-b the tumor location is detected with a minimum size of 0.3mm and absorption SAR_{max} 8.717 W/Kg depend on the location of the tumor in the SAR plateau with the respect to the x, y plan of the slice layer.

TABLE 2
THE MAXIMUM SAR FOR DIFFERENT TUMOR SIZES AT NOMINATED LOCATION Q = (-30, 0, 60), AND MSPA AT Θ =0°

tumor size (mm)	Estimated results				δ	Deviation			Decision
	Max SAR (W/Kg)	x	y	z		δx	δy	δz	
0.1	27.36	-56.5	-1.41	78.35	±0.05	26.5	1.41	18.4	outside breast
0.2	27.36	-56.5	-1.41	78.35	±0.1	26.5	1.41	18.4	
0.3	8.717	-29.9	-0.035	60.1	±0.15	0.1	0.04	0.1	inside tumor
0.4	7.028	-29.85	-0.087	60.1	±0.2	0.15	0.09	0.1	
0.5	5.838	-29.9	-0.02	60.2	±0.25	0.1	0.02	0.2	
0.6	4.891	-30	0	60	±0.3	0	0	0	
0.7	3.41	-30	0	60	±0.35	0	0	0	
0.8	3.666	-30	0	60	±0.4	0	0	0	
0.9	4.056	-30	0	60	±0.45	0	0	0	
1	4.284	-30	0	60	±0.5	0	0	0	
2	4.157	-30.5	0	60	±1	0.5	0	0	
3	7.247	-31	0	60	±1.5	1	0	0	
4	20.16	-31.5	0	60	±2	1.5	0	0	
5	78.22	-31.5	0	60	±2.5	1.5	0	0	

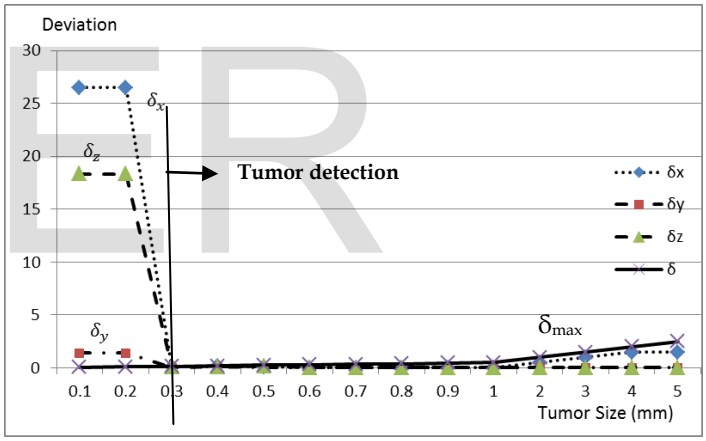

Fig. 5. Tumor size versus maximum SAR and deviation

Figure 5, is derived from the result in table-2. It's constructed for the deviation δmax, δx, δ_y, and δ_z to clarify which tumor size can be detected (δ ≤ δmax). For any deviation values δ above the δmax line there is no detection for such tumor, and for δ(s) under the δmax line, the tumor can be detected. From the table and δ grave, it is seen that the tumor of size less than 0.3mm (vertical dotted line) will not be detected. Whereas tumor of size equals 0.3mm or greater must be detected. Then 0.3mm is the smallest tumor size detection with SAR_{max} equal 8.717 W/Kg in this case.

Consider the detected smallest tumor size ($r_{t\text{-}min}$) for the given slice layer position, and its corresponding absorption (SAR_{max}), construct same parameters for different scan angle θ=90°, 180°, and 270°.

Table 3, shows the result of scanning the MSPA around the slice layer position Z_s=70mm.

TABLE 3
THE MAXIMUM SAR AND THE MINIMUM TUMOR SIZES DETECTION AT Z_{SLICE} = 80

Result \ θ	θ =0°	θ =90°	θ =180°	θ =270°
$r_{t\,min}$ (mm)	0.3	0.3	0.3	0.3
SAR_{max} (W/Kg)	8.717	3.92	1.45	3.9

From table 3 it is found that the absorption SAR_{max} value decreases as scan angle increases from 0° to 180° and then retains its value from 180° to 360°. It is worth to note that the absorption SAR_{max} value is symmetric about the zero scan angles.

5.2 Experiment-2.

Consider antenna position for the second slice layer is Z_{slice}=70mm, figure 3-a shows the obtained solution results for anthropomorphic lobe body profile and direction, figure 3-b shows the SAR plateau distribution as well as the spike of the absorption SAR_{max} detectable location at rotation angle θ=0°.

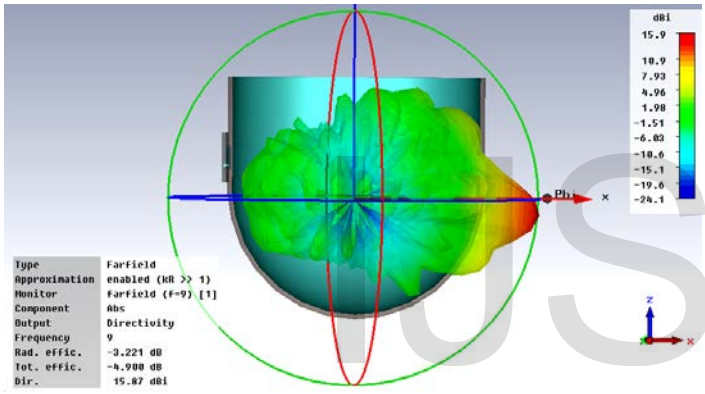

(a): The anthropomorphic far-field

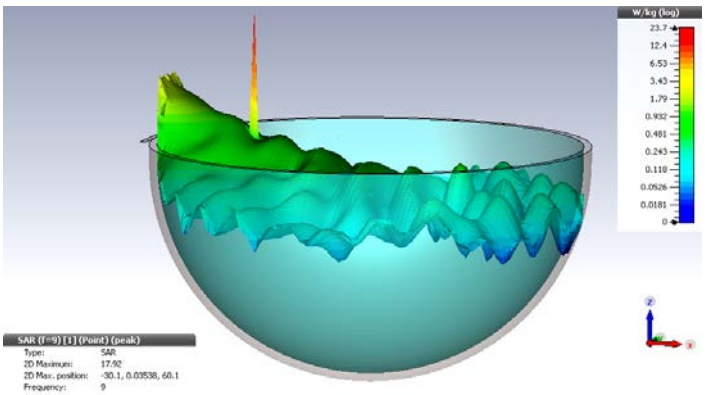

(b): SAR distribution profile for minimum size.

Fig. 6. The anthropomorphic far-field and SAR_{max} at minimum tumor size.

From fig. 6 it is evident that the anthropomorphic lobe body is directed downwards for bottom with the tilt angle Φ=-10, and from fig. 6-b the tumor location is detected with a minimum size of 0.3mm and absorption SARmax 17.92 W/Kg depend on the location of the tumor in the SAR plateau with the respect to the x, y plan of the slice layer.

Table 4 gives the results for different tumor size according to the criteria for detectable tumor where the absorption SAR_{max} inside tumor spheres.

TABLE 4
THE MAXIMUM SAR FOR DIFFERENT TUMOR SIZES AT NOMINATED LOCATION Q = (-30, 0, 60), MSPA AT Z_{SLICE}= 70, AND Θ= 0°.

tumor size (mm)	Simulated results				δ	Deviation			Decision
	Max SAR (W/Kg)	x	y	z		δx	δy	δz	
0.1	27.48	-56.5	-1.41	68.35	±0.05	26.5	1.41	8.3	outside breast
0.2	27.48	-56.5	-1.41	63.35	±0.1	26.5	1.41	3.4	
0.3	17.92	-30.1	-0.035	60.1	±0.15	0.1	0.04	0.1	inside tumor
0.4	16	-30	0	60	±0.2	0	0	0	
0.5	14.13	-30	0	60	±0.25	0	0	0	
0.6	12.29	-30	0	60	±0.3	0	0	0	
0.7	8.525	-30	0	60	±0.35	0	0	0	
0.8	9.216	-30	0	60	±0.4	0	0	0	
0.9	9.894	-30	0	60	±0.45	0	0	0	
1	10.61	-30	0	60	±0.5	0	0	0	
2	10.66	-30	0	59.5	±1	0	0	0.5	
3	17	-31	0	60	±1.5	1	0	0	
4	45.6	-31.5	0	60	±2	1.5	0	0	
5	179.1	-31.5	0	60	±2.5	1.5	0	0	

Table 5, shows the result of scanning the MSPA around the slice layer position Z_s=70mm.

TABLE 5
THE MAXIMUM SAR AND THE MINIMUM TUMOR SIZES DETECTION AT Z_{SLICE} = 70

Result \ θ	θ =0°	θ =90°	θ =180°	θ =270°
$r_{t\,min}$ (mm)	0.3	0.3	4	0.3
SAR_{max} (W/Kg)	17.92	4.23	7.49	4.23

From table 5 it is found that the absorption SAR_{max} value decreases as scan angle increases from 0° to 180° and then retains its value from 180° to 360°. It is worth to note that the absorption SAR_{max} value is symmetric about the zero scan angles.

Notice: it is worth to note that for this case where the slice layer Z_s= 70mm the equipped area of the anthropomorphic lobe body profile is greater than for the slice layer Z_s=90mm.

5.3 Experiment-3

Consider antenna position for the third slice layer is Z_{slice}=55mm, figure 6-a shows the obtained solution results for anthropomorphic lobe body profile and direction, figure 6-b shows the SAR plateau distribution as well as the spike of the absorption SAR_{max} detectable location at rotation angle θ=0°.

Table 6 gives the results for different tumor size according to the criteria for detectable tumor where the absorption SAR_{max} inside tumor spheres.

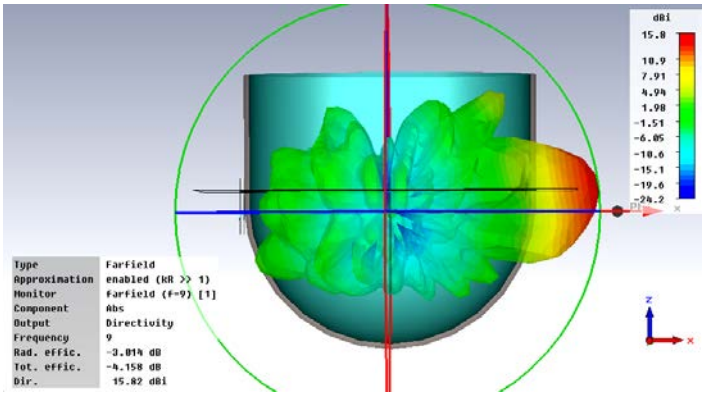

(a): The anthropomorphic far-field structure.

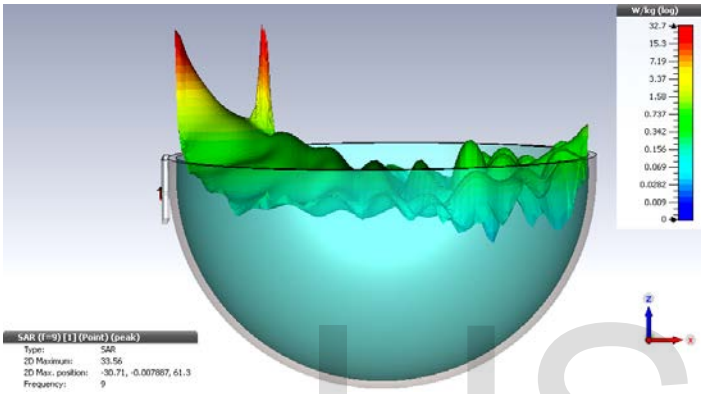

(b): SAR distribution profile for minimum size.

Fig. 7. The anthropomorphic far-field and SAR_{max} at minimum tumor size.

From fig. 7 it is evident that the anthropomorphic lobe body is directed towards the tumor, the tilt angle $\Phi \approx 0$, and from fig. 7-b the tumor location is detected with a minimum size of 3mm and absorption SARmax 33.56 W/Kg depend on the location of the tumor in the SAR plateau with the respect to the x, y plan of the slice layer.

TABLE 6
THE MAXIMUM SAR FOR DIFFERENT TUMOR SIZES AT NOMINATED LOCATION Q = (-30, 0, 60), MSPA AT Z_{SLICE} = 55, AND $\Theta = 0^{O}$.

tumor size (mm)	Simulated results				δ	Deviation			Decision
	Max SAR (W/Kg)	x	y	z		δx	δy	δz	
0.1	39.96	-51.6	-4.85	45.9	±0.05	21.6	4.85	14.1	outside breast
0.2	74.09	-51.7	-8.94	48.95	±0.1	21.69	8.94	11.1	
0.3	38.93	-53	-0.035	59.9	±0.15	23	0.04	0.1	
0.4	33.89	-53	0	59.96	±0.2	23	0	-0	
0.5	33.73	-53	0	60	±0.25	23	0	0	
0.6	32.73	-53	0	60	±0.3	23	0	0	
0.7	33.18	-53	0.98	60	±0.35	23	0.98	0	
0.8	33.34	-53	0.98	60	±0.4	23	0.98	0	
0.9	33.3	-53	0.98	60	±0.45	23	0.98	0	
1	33.34	-53	0.98	60	±0.5	23	0.98	0	
2	34.23	-53	1	60	±1	23	1	0	
3	33.56	-30.7	-0.007	61.3	±1.5	0.71	0.01	1.3	inside tumor
4	77.27	-31	0	60.9	±2	1	0	0.9	
5	307	-31.5	0	60	±2.5	1.5	0	0	

Table 7, shows the result of scanning the MSPA around the slice layer position Z_s=55mm.

TABLE 7
THE MAXIMUM SAR AND THE MINIMUM TUMOR SIZES DETECTION AT Z_{SLICE} = 55

Result \ θ	θ =0°	θ =90°	θ =180°	θ =270°
$r_{t\text{-}min}$ (mm)	3	6	5	6
SAR_{max} (W/Kg)	33.56	35.14	57.35	35.09

From table 7 it is found that the absorption SAR_{max} value decreases as scan angle increases from 0° to 180° and then retains its value from 180° to 360°. It is worth to note that the absorption SAR_{max} value is symmetric about the zero scan angles.

Notice: it is worth to note that for this case where the slice layer Z_s= 55mm the equipped area of the anthropomorphic lobe body profile is almost symmetric about the tilt angle Φ=0°.

5.4 Experiment-4.

Consider antenna position for the fourth slice layer is Z_{slice}=40mm, figure 7-a shows the obtained solution results for anthropomorphic lobe body profile and direction, figure 7-b shows the SAR plateau distribution as well as the spike of the absorption SAR_{max} detectable location at rotation angle θ=0°.

Table 8 gives the results for different tumor size according to the criteria for detectable tumor where the absorption SAR_{max} inside tumor spheres.

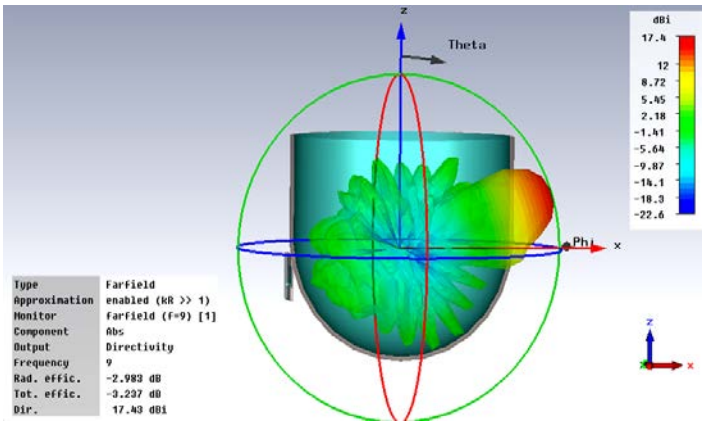

(a): The anthropomorphic far-field structure.

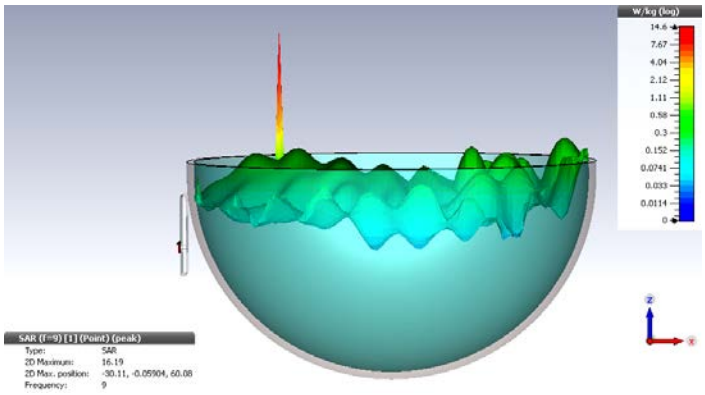

(b): SAR distribution profile for minimum size.

Fig. 8. The anthropomorphic far-field and SAR_{max} at minimum tumor size.

From fig. 8 it is evident that the anthropomorphic lobe body is directed upwards for upper with the tilt angle Φ=10, and from fig. 8-b the tumor location is detected with a minimum size of 0.3mm and absorption SARmax 16.19 W/Kg depend on the location of the tumor in the SAR plateau with the respect to the x, y plan of the slice layer.

TABLE 8
The Maximum SAR For Different Tumor Sizes At Nominated Location Q = (-30, 0, 60), MSPA At Z_{SLICE} = 40, and Θ= 0^O.

tumor size (mm)	Estimated results				δ_{max}	Deviation			Decision
	Max SAR (W/Kg)	x	y	z		δx	δy	δz	
0.1	99.25	-52.41	0.046	39.82	±0.05	22.41	0.05	20.2	outside breast
0.2	56.32	-56.5	-1.41	38.35	±0.1	26.5	1.41	21.7	
0.3	16.19	-30.11	-0.06	60.08	±0.15	0.11	0.06	0.08	inside tumor
0.4	12.83	-30.15	-0.08	60.1	±0.2	0.15	0.09	0.1	
0.5	10.28	-30.14	-0.02	60.2	±0.25	0.14	0.02	0.2	
0.6	9.4	-30.19	-0.07	60.2	±0.3	0.19	0.07	0.2	
0.7	6.741	-30.15	-0.23	60.2	±0.35	0.15	0.23	0.2	
0.8	6.728	-30.3	-0.17	60.2	±0.4	0.3	0.17	0.2	
0.9	7.13	-30.34	-0.19	60.3	±0.45	0.34	0.2	0.3	
1	7.536	-30.34	-0.16	60.3	±0.5	0.34	0.16	0.3	
2	6.735	-30.5	0	60.5	±1	0.5	0	0.5	
3	10.03	-31	0	60.5	±1.5	1	0	0.5	
4	25.5	-31.5	0	60.5	±2	1.5	0	0.5	
5	69.92	-31	0	59	±2.5	1	0	1	

Table 9, shows the result of scanning the MSPA around the slice layer position Z_s=70mm.

TABLE 9
The Maximum SAR And The Minimum Tumor Sizes Detection At Z_{SLICE} = 40

Result \ θ	θ =0°	θ =90°	θ =180°	θ =270°
$r_{t\ min}$ (mm)	0.3	0.3	0.3	0.3
SAR_{max} (W/Kg)	16.19	7.95	6.11	7.94

From table 9 it is found that the absorption SAR_{max} value decreases as scan angle increases from 0° to 180° and then retains its value from 180° to 360°. It is worth to note that the absorption SAR_{max} value is symmetric about the zero scan angles.

Notice: it is worth to note that for this case where the slice layer Z_s= 40mm the equipped area of the anthropomorphic lobe body profile is larger than for the slice layer Z_s=90mm.

5.5 Experiment-5

Consider antenna position for the fifth slice layer is Z_{slice}=20mm, figure 8-a shows the obtained solution results for anthropomorphic lobe body profile and direction, figure 8-b shows the SAR plateau distribution as well as the spike of the absorption SAR_{max} detectable location at rotation angle θ=0°.

Table 10 gives the results for different tumor size according to the criteria for detectable tumor where the absorption SAR_{max} inside tumor spheres.

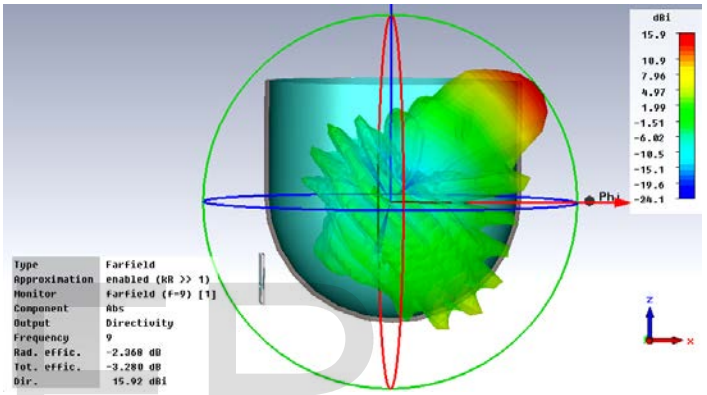

(a): The anthropomorphic far-field structure.

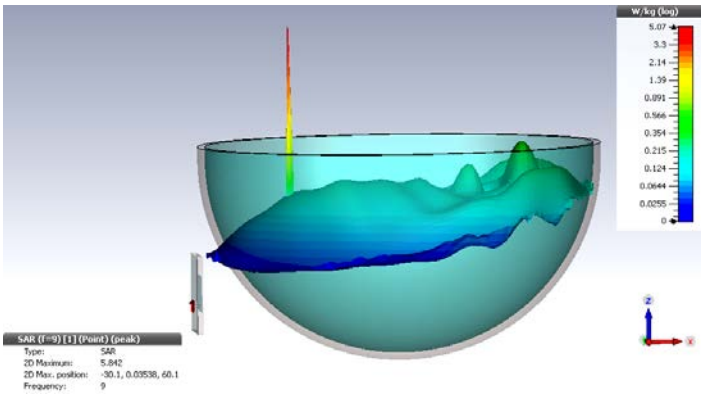

(b): SAR distribution profile for minimum size.

Fig. 9. The anthropomorphic far-field and SAR_{max} at minimum tumor size.

From fig. 9 it is evident that the anthropomorphic lobe body is directed upwards for upper with the tilt angle Φ=30, and from fig. 9-b the tumor location is detected with a minimum size of 0.3mm and absorption SARmax 5.842 W/Kg depend on the location of the tumor in the SAR plateau with the respect to the x, y plan of the slice layer.

TABLE 10

The Maximum SAR For Different Tumor Sizes At Nominated Location Q = (-30, 0, 60), MSPA At Z_{SLICE}=20, and Θ= 0^O.

tu-mor size (mm)	Simulated results				δ	Deviation			Deci-sion
	Max SAR (W/Kg)	x	y	z		δx	δy	δz	
0.1	74.33	-56.5	-1.41	18.35	±0.05	26.5	1.41	41.7	outside breast
0.2	74.33	-56.5	-1.41	18.35	±0.1	26.5	1.41	41.7	
0.3	5.842	-30.1	0.03	60.1	±0.15	0.1	0.03	0.1	inside tumor
0.4	4.76	-30.15	0.086	60.1	±0.2	0.15	0.09	0.1	
0.5	3.78	-30.14	0.02	60.2	±0.25	0.14	0.02	0.2	
0.6	3.56	-30.19	0.07	60.2	±0.3	0.19	0.07	0.2	
0.7	2.549	-30.15	-0.22	60.2	±0.35	0.15	0.22	0.2	
0.8	2.586	-30.3	-0.17	60.2	±0.4	0.3	0.17	0.2	
0.9	2.728	-30.34	-0.2	60.2	±0.45	0.34	0.2	0.2	
1	2.9	-30.34	-0.15	60.3	±0.5	0.34	0.15	0.3	
2	2.42	-29.5	0	59.5	±1	0.5	0	0.5	
3	3.42	-31	0	60.5	±1.5	1	0	0.5	
4	7.877	-31.5	0	60.5	±2	1.5	0	0.5	
5	28.3	-31.5	0	60	±2.5	1.5	0	0	

Table 11, shows the result of scanning the MSPA around the slice layer position Z_s=70mm.

TABLE 11
THE MAXIMUM SAR AND THE MINIMUM TUMOR SIZES DETECTION AT Z_{SLICE} = 20

Result \ θ	θ =0°	θ =90°	θ =180°	θ =270°
$r_{t\,min}$ (mm)	0.3	0.3	0.3	0.3
SAR_{max} (W/Kg)	5.84	5.679	9.457	5.604

From table 11 it is found that the absorption SAR_{max} value decreases as scan angle increases from 0° to 180° and then retains its value from 180° to 360°. It is worth to note that the absorption SAR_{max} value is symmetric about the zero scan angles.

4.6 Experiment-6.

Consider antenna position for the sixth slice layer is Z_{slice} at the bottom (nipple), figure 9-a shows the obtained solution results for anthropomorphic lobe body profile and direction, figure 9-b shows the SAR plateau distribution as well as the spike of the absorption SAR_{max} detectable location at rotation angle θ=0°.

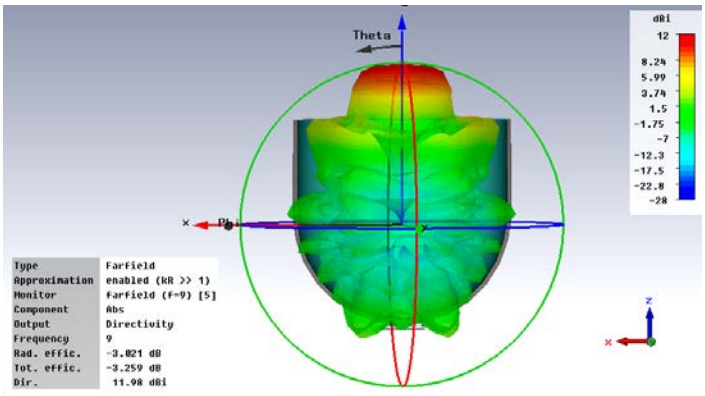

(a): The anthropomorphic far-field structure.

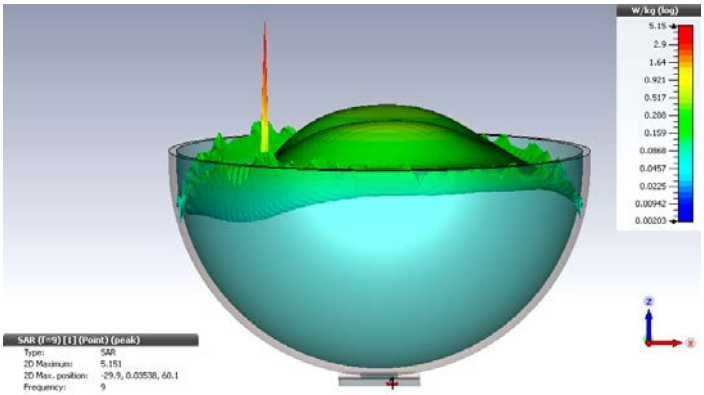

(b): SAR distribution profile for minimum size.

Fig. 10. The anthropomorphic far-field and SAR_{max} at minimum tumor size.

From fig. 10 it is evident that the anthropomorphic lobe body is directed upwards for upper with the tilt angle Φ=90, and from fig. 10-b the tumor location is detected with a minimum size of 0.3mm and absorption SARmax 5.15 W/Kg depend on the location of the tumor in the SAR plateau with the respect to the x, y plan of the slice layer.

Table 12 gives the results for different tumor size according to the criteria for detectable tumor where the absorption SAR_{max} inside tumor spheres.

TABLE 12
THE MAXIMUM SAR FOR DIFFERENT TUMOR SIZES AT NOMINATED LOCATION Q = (-30, 0, 60), AND MSPA AT THE BOTTOM OF THE CHAMBER.

tumor size (mm)	Simulated results				δ	Deviation			Decision
	Max SAR (W/Kg)	x	y	z		δx	δy	δz	
0.1	25.24	-4.2	0	3.67	±0.05	25.8	0	56.3	outside breast
0.2	25.24	-4.2	0	3.67	±0.1	25.8	0	56.3	
0.3	5.15	-29.9	0.035	60.1	±0.15	0.09	0.04	0.1	inside tumor
0.4	4.195	-29.8	0.087	60.1	±0.2	0.15	0.09	0.1	
0.5	3.55	-29.8	0.01	60.13	±0.25	0.18	0.01	0.13	
0.6	3.04	-29.8	0.12	60.16	±0.3	0.2	0.12	0.16	
0.7	2.16	-29.8	0.26	60.17	±0.35	0.15	0.26	0.17	
0.8	2.15	-29.7	0.17	60.2	±0.4	0.3	0.17	0.2	
0.9	2.34	-29.7	0.19	60.23	±0.45	0.3	0.19	0.23	
1	2.48	-30	0	60	±0.5	0	0	0	
2	2.34	-29.5	0	60	±1	0.5	0.00	0	
3	2.99	-28.6	-0.62	60.1	±1.5	1.4	0.62	0.1	
4	7.13	-28.2	-0.034	60.8	±2	1.8	0.03	0.8	
5	15.67	-28.5	0	60.1	±2.5	1.5	0	0.1	

Notice: it is worth to note that for this case where the slice layer Z_s at the bottom (nipple), the equipped area of the anthropomorphic lobe body profile is almost occupied the whole breast volume.

Considering the mention of experiments and results, table

13, shows the effect of slice layers positioning and antenna scan angle effect as well as the tilt angle shift.

TABLE 13
COMPARISON TABLE FOR DIFFERENT SLICES AND ANGLES.

Slice (mm)	θ / Result	θ =0°	θ =90°	θ =180°	θ =270°	Φ
90	$r_{t\text{-}min}$ (mm)	0.3	0.3	0.3	0.3	-30°
	SAR_{max} (W/Kg)	2.265	5.32	1.503	5.32	
80	$r_{t\text{-}min}$ (mm)	0.3	0.3	0.3	0.3	-20°
	SAR_{max} (W/Kg)	8.717	3.92	1.45	3.9	
70	$r_{t\text{-}min}$ (mm)	0.3	0.3	4	0.3	-10°
	SAR_{max} (W/Kg)	17.92	4.23	7.49	4.23	
55	$r_{t\text{-}min}$ (mm)	3	6	5	6	0°
	SAR_{max} (W/Kg)	33.56	35.14	57.35	35.09	
40	$r_{t\text{-}min}$ (mm)	0.3	0.3	0.3	0.3	10°
	SARmax (W/Kg)	16.19	7.95	6.11	7.94	
20	$r_{t\text{-}min}$ (mm)	0.3	0.3	0.3	0.3	30°
	SARmax (W/Kg)	5.84	5.679	9.457	5.604	
0	$r_{t\text{-}min}$ (mm)	0.3	0.3	0.3	0.3	40°
	SARmax (W/Kg)	3.248	5.104	8.09	5.042	
Bottom (nipple)	$r_{t\text{-}min}$ (mm)	0.3				90°
	SARmax (W/Kg)	5.15				

From this table its seen that the anthropomorphic lobe body direction depends on the MSPA position along the major axis of the modeled breast. Also, it is evident that the bottom (nipple) position is the most suitable inspection method for smallest tumor detection.

5 CONCLUSION

The simplicity of MSPA design configuration and its position for axially and rotation inspection for tumor detection.

The positioning of MSPA against breast slice layer shows that the far-field anthropomorphic lobe body allows detecting tumor with different tilt angle as well as the scan angle for detection of tumor smallest detectable size down to 0.3mm. the tilt angle is sensitive to and on the volumetric conductivity of the lobe with respect to total volume conductivity.

Also, it is noticed that as antenna positioning moves towards the bottom (nipple) the far-field anthropomorphic lobe body covers the whole breast area. Moreover, the SAR plateau depends drastically on breast volume and the maximum detectable SAR in the tumor is a function of the SAR plateau value at the tumor location.

It is of importance to mention that the far-field profile probably seems to suffer from edge effect like at the top of the proposed model.

REFERENCES

[1 Mazhar B. Tayel, Hazem A. Elfaham "microwave SAR as a Tool for tumor Determination" ICCES 2016 the 11th International conference of computer engineering and systems, December 2016.

[2] Mazhar B. Tayel, Hazem A. Elfaham "A proposed algorithm to determine breast smallest tumor location and size" International Journal of Scientific & Engineering Research, Volume 8, Issue 1, January-2017.

[3] Maryann Verrillo, Diane Schnitzler "Minimally Invasive Treatments for Breast Cancer Interventional Radiology Treatments Offer New Options and Hope to Patients Who Are Not Good Surgical Candidates," Society of International radiology, December 2004.

[4] N. Hoogerbrugge, et al, "The impact of a false-positive MRI on the choice for mastectomy in BRCA mutation carriers is limited," Annals of Oncology, vol. 19, no. 4, pp. 655-659, 2008.

[5] Andresen Singh, Dr. V.S. Tripathi "Microstrip Patch Antenna and its Applications" IJCTA SEPT-OCT 2011.

[6] http://www.cst.com. CST Microwave Studio 2014.

[7] Ponnuraj Kirthi Priya & S. Poonguzhali, "Detection of Breast Cancer Using Microwave Absorption Loss" International Conference on Electronics and Communication Engineering, 20th, May 2012, Bangalore, ISBN: 978-93-81693-29-2, Chennai, India.

[8] ENGY Alaa El Din Hanafy, Abdelmegid Allam "Diagnosis of Breast Tumors using a PIFA antenna," International Journal of Computer and Information Technology (ISSN: 2279 – 0764) Volume 03 – Issue 05, September 2014.

[9] V.Karthikeyan and V.J.Vijayalakshmi "RADIATION PATTERN OF PATCH ANTENNA WITH SLITS" International Journal on Information Theory (IJIT), Vol.3, No.1, January 2014, India.

[10] R.Sreeja, E.Vinodhini, S.Vanaja, Dr. S. Poonguzhali "Radar-Based Breast Cancer Detection Using SAR" International Journal of Advanced Research in Electrical, Electronics and Instrumentation Engineering, Vol. 3, Special Issue 2, April 2014.

[11] Omar K. Hammouda, Prof. Dr. A. M. M. Allam "Diagnosis Of Oral Cancers Using Implanted Antennas" Scientific Cooperations International Workshops on Electrical and Computer Engineering Subfields 22-23 August 2014, Koc University, ISTANBUL/TURKEY.

[12] Online Help/cst_studio_suite_help.htm.